Non-muscle Myosin Type-II Localization in the Mouse Intestinal Villi is Altered by B-Type Natriuretic Peptide

Anteneh Addisu *, Yunus E. Dogan, Darrice Montgomery, Leeyu Addisu, Abdel A Alli

Posted Date: 1 May 2023

doi: 10.20944/preprints202305.0012.v1

Keywords: Non-Muscle Myosin; BNP; GI epithelia; Apical junctional complex; Absorption

Article

Non-Muscle Myosin Type-II Localization in the Mouse Intestinal Villi is Altered by B-Type Natriuretic Peptide

Anteneh Addisu [1,2,*], Yunus E. Dogan [2], Darrice Montgomery [2], Leeyu Addisu [2] and Abdel A. Alli [2,3,*]

[1] Department of Molecular Pharmacology and Physiology University of South Florida College of Medicine, Tampa Fl
[2] Department of Physiology and Aging University of Florida College of Medicine, Gainesville Fl
[3] Department of Medicine Division of Nephrology, Hypertension, and Renal Transplantation, University of Florida College of Medicine, Gainesville Fl
* Correspondence: Dr. Anteneh Addisu; aaddisu@usf.edu; Tel.: +352-362-6104

Abstract: Our prior studies have shown that B type Natriuretic Peptide (BNP) decreases absorption from the gastrointestinal (GI) tract. Since non-muscle myosin-type II (NMM-II) is known to have a role in epithelial tight junction regulation, we aimed to test whether BNP has an effect on the localization and expression of NMM-II in the intestinal villi. We treated wild type mice with a 10 ng/g intravenous bolus of BNP followed by infusion of BNP at 1ng/g/minute vs. vehicle control. The mice were then euthanized and intestinal tissue isolated and sectioned. The tissue was immune-stained for NMM-II and examined using fluorescence microscopy. The tissue section not treated with antibody to NMM-II was used as a methodological control to evaluate the non-specific binding. Scanning electron micrographic images were taken to compare structural differences between the two groups. Western blotting was performed to compare the regional protein expression of NMM-II and associated proteins including smooth muscle actin, kinesin, and E cadherin in small intestinal tissue between BNP vs. vehicle infused mice. Fluorescence microscopy revealed markedly increased localization of NMM-II at the crypts and core of intestinal villi of the jejunum, ileum and colon of BNP treated mice compared to vehicle. Transmission electron microscopy revealed that the microvilli of BNP treated mice assumed the distinctive appearance of 'relaxed' microvilli compared to vehicle. Such decrease in contractility was previously shown to decrease para-cellular permeability of epithelia. Our observation indicates that BNP alters the localization of NMM-II in intestinal villi and makes the intestinal villi structures assume a state of decreased permeability of the apical junctional complex. Further characterization of this process and understanding the specific mediators involved could lead to the identification of novel therapeutic targets for various disease states such as heart failure and malabsorption.

Keywords: non-muscle myosin; BNP; GI epithelia; apical junctional complex; absorption

1. Introduction

Non-muscle myosins (NMM) are part of the class II myosin isoforms that are widely distributed and expressed in eukaryotic cells. In non-muscle cells, NMM type-II (NMM-II) associates with and regulates the organization of actin filaments in a manner that is distinct from skeletal muscle actomyosin interaction [1–3]. Some of the various functions of such NMM mediated mechanotransduction include cytoskeletal tension, cell division, chemotaxis, polarity, cell motility and maintaining of the cell shape [2–7]. NMM-II is also one of several proteins involved in cell attachment at the apical junctional complex of epithelia, which includes tight and adherens junctions (AJ) and constitutes the adhesive belt that links epithelial cells [8]. More specifically, NMM-II is known to localize on the cytoplasmic side of the tight junction in a circumferential ring sometimes referred to as the actin belt. NMM-II mediated contraction of this circumferential ring of the tight junctions provide one mechanism for the regulation of paracellular permeability of intestinal epithelia [9–11]. This was further supported by studies performed in various types of epithelia (of the

 doi:10.20944/preprints202305.0012.v1

kidney, bladder and intestinal mucosa) that have confirmed changes in permeability that are regulated by phosphorylation related contractile changes at the apical junctional complex. These changes are thought to primarily regulate paracellular movement of water and small- molecular weight solutes [12–14]. Such paracellular permeability of tight junctions varies among different tissues and also within the same type of epithelia depending on the type of a particular stimuli and on whether a small molecule solute or a large macromolecule is being allowed to pass through the epithelial barrier [15]. Furthermore, the integrity and stability of the epithelial barrier is dependent on the regulation of NMM and other cell junction associated proteins including epithelial cadherin (E-cadherin), smooth muscle actin, and kinesin. E-cadherin plays an essential role in the formation of AJ and associates with several proteins that are involved in linking the actin cytoskeleton at the plasma membrane [8]. The actin cytoskeletal structure consists of a myriad of proteins including actin and proteins such as the myristoylated alanine rich C kinase substrate (MARCKS) and filamin that crosslink actin. The actin cytoskeleton plays an important role in maintaining the dynamic organization of tight junctions [16] and it serves as an organizing center that allow for the regulation of membrane proteins [17–19]. Microtubules have also been shown to regulate epithelial tight junction structure and function [20]. The microtubule-dependent molecular motors, kinesins were also shown to be enriched at the apical junctional complex (AJC) which regulates cell polarity, intercellular adhesion, and paracellular permeability [21].

Our prior studies have shown that BNP decreases intestinal absorption in mice [22,23]. The mechanism of these effects of BNP in the GI tract is unknown. However, some of the other known biological effects of BNP are mediated through mechanisms that result in smooth muscle cell relaxation [24–26]. We thus aimed to test whether BNP would have an effect on the expression and localization of NMM-II in the contractile structures of the intestinal villi, thereby suggesting an effect on the contractility of the villi and hence indicating a possible mechanism for the previously observed effect of BNP on gastric emptying and intestinal absorption. In addition, since prior transmission electron micrographic (TEM) imaging of intestinal villi has shown contractile changes at the level of the AJ that correlated with various degrees of epithelial permeability, we also obtained TEM imaging of BNP treated vs. control intestinal epithelial tissue to investigate the structural changes that could be due to BNP.

We present here whole mouse and tissue derived immunohistochemical imaging and biochemical data showing the effect of BNP on the localization of NMMII in the intestinal villi. Additionally, the significance of these change are discussed.

2. Results

2.1. Increased Localization of NMM-II along the Crypt and Core of the Intestinal Villi of BNP Treated Mice

Intestinal tissue of jejunum, ileum and colon from BNP treated mice revealed increased localization of NMM-II along the crypt and core of the intestinal villi compared to tissue from vehicle control mice as shown in Figure 1.

Preprints (www.preprints.org) | NOT PEER-REVIEWED | Posted: 1 May 2023 doi:10.20944/preprints202305.0012.v1

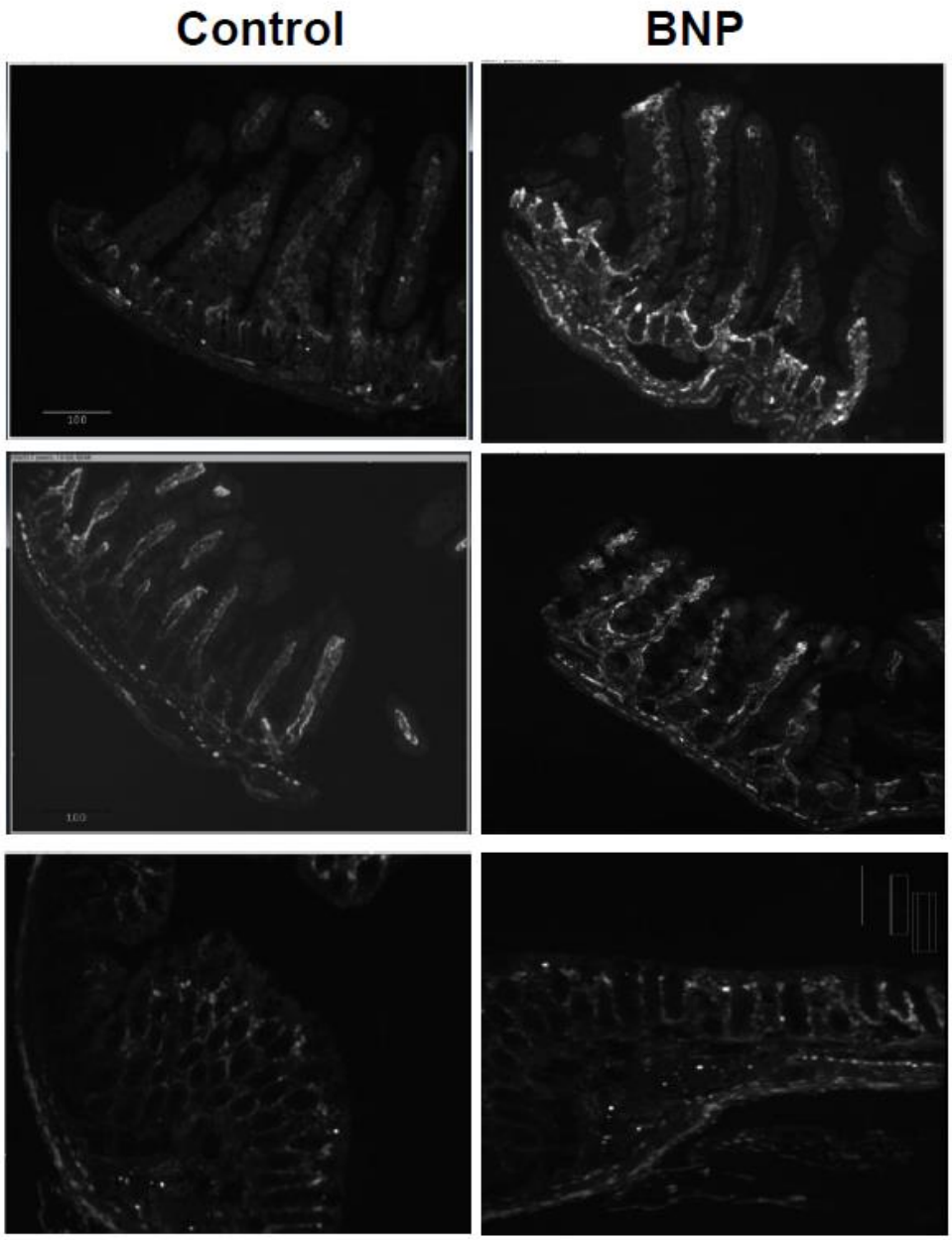

Figure 1. Immunohistochemical analysis of 3µm sections of NMM-II in intestinal tissue. Intestinal tissue (J-Jejunum, I-Ileum and C-Colon) were fixed and stained with antibodies against non-muscle myosin II B in control vs. BNP treated mice. Tissue from BNP treated mice shows increased localization of NMM-II along the core and crypt of the intestinal epithelial villi with intensity of localization decreasing from ileum to colon.

This increased localization is most pronounced in the proximal gut (the ileum) compared to distal gut (colon). Our negative control image as shown in Figure 2 shows that there is very little (if any) background binding.

Preprints (www.preprints.org) | NOT PEER-REVIEWED | Posted: 1 May 2023 doi:10.20944/preprints202305.0012.v1

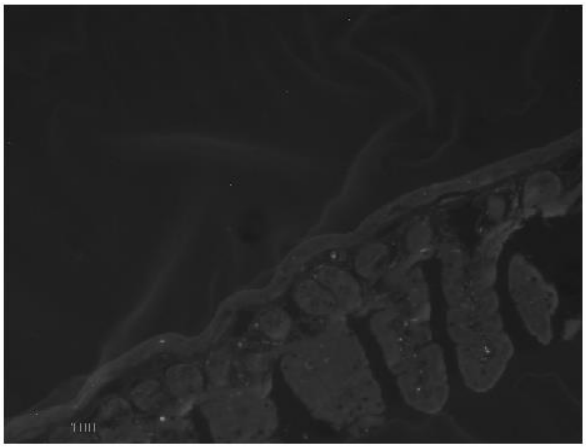

Figure 2. Negative control immunohistochemistry experiment. Ileal tissue with omission of the primary antibody shows very limited or no background binding.

2.2. Microvilli from BNP Treated mice Assume a Relaxed State

As shown in Figure 3, TEM imaging shows that the villi/microvilli of intestinal epithelial tissue from BNP treated mice lost the typical 'fanning' appearance of contracting microvilli and assumed a 'relaxed' state.

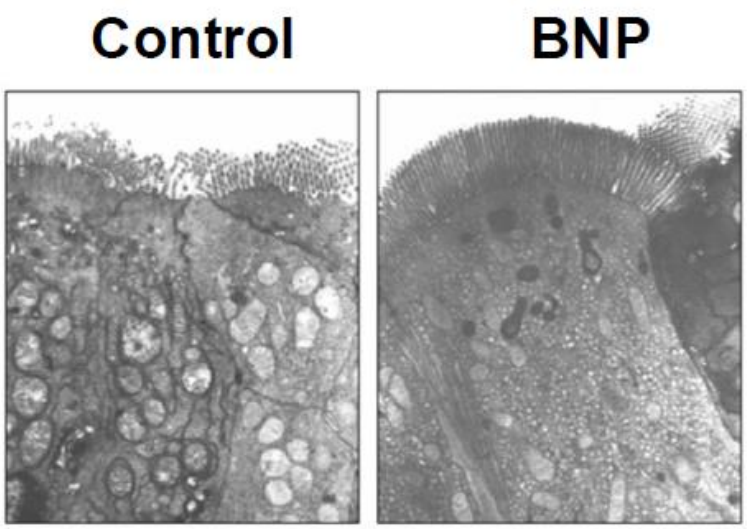

Figure 3. Thin-section transmission electron micrograph of representative ileal epithelial tissue from control vs BNP treated mice BNP treated tissue epithelium shows microvilli that have lost the usual separation ('fanning') which is seen in contracting microvilli. X 10,000.

2.3. BNP infusion Attenuates NMM-II Protein Expression Mainly in the Jejunum

To determine if BNP infusion affects the protein expression of NMM-II in different segments of the small intestine, we dissected and homogenized the main segments of the small intestine. Western blot and densitometric analyses show protein expression of NMM-II is greater in the jejunum and ileum compared to its expression in the duodenum. Next, we examined regional protein expression levels of NMM-II in intestinal tissue from mice infused with either BNP or vehicle. Figure 4A,B shows NMM-II protein expression in the jejunum is significantly reduced in mice infused with BNP compared to mice that received vehicle.

Preprints (www.preprints.org) | NOT PEER-REVIEWED | Posted: 1 May 2023 doi:10.20944/preprints202305.0012.v1

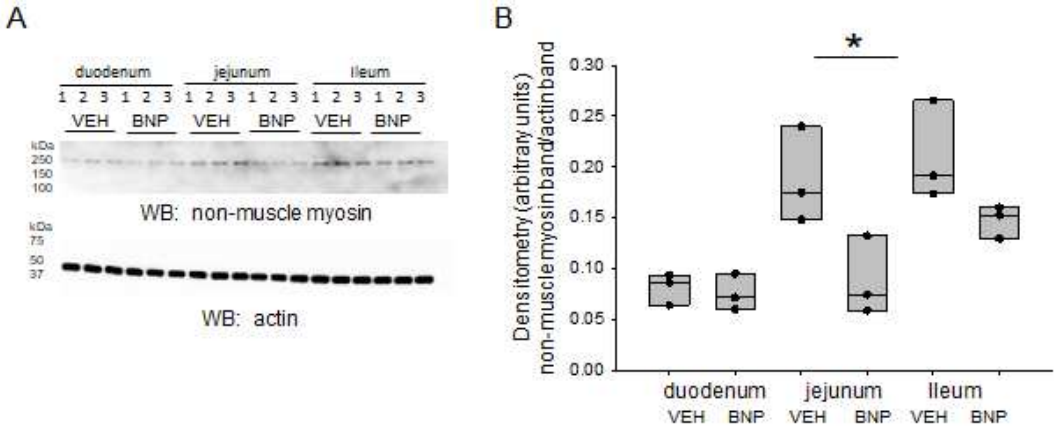

Figure 4. Western blot and densitometric analysis of NMM in the small intestine of mice infused with BNP or vehicle. A. Western blot showing endogenous levels of NMM protein expression (top blot) in the duodenum, jejunum. and ileum and the effect of BNP infusion compared to the infusion of vehicle (VEH). Western blot for actin used to assess lane loading. B. Densitometric analysis of the immunoreactive NMM band in the Western blot in panel A normalized to the actin band. * represents a p-value<0.05.

2.4. BNP Infusion does not Alter Smooth Muscle Actin Protein Expression in the Small Intestine

Since smooth muscle actin is an integral part of the contractile sarcomeric belt at the AJC and associates with NMM, we investigated whether BNP infusion alters its density in different segments of the small intestine. Western blot and densitometric analysis did not show any appreciable differences in smooth muscle protein expression in the duodenum, jejunum, or ileum for mice infused with BNP compared to vehicle (Figure 5).

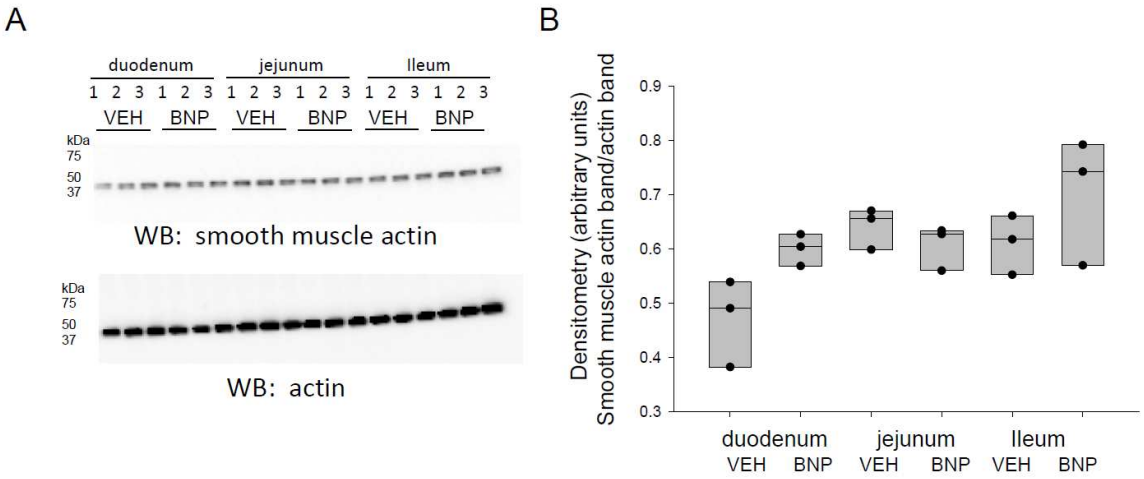

Figure 5. Western blot and densitometric analysis of smooth muscle actin in the small intestine of mice infused with BNP or vehicle. A. Western blot showing endogenous levels of smooth muscle actin protein expression (top blot) in the duodenum, jejunum. and ileum of mice infused with BNP or vehicle (VEH). Western blot for actin used to assess lane loading. B. Densitometric analysis of the immunoreactive smooth muscle actin band in the Western blot in panel A normalized to the actin band.

2.5. E-cadherin Protein Expression is Attenuated in Distal Parts of the Small Intestine after BMP Infusion

E-cadherin is another protein that is known to associate with NMM. Therefore, we investigated whether BNP infusion, compared to infusion of vehicle alters E-cadherin protein expression in

Preprints (www.preprints.org) | NOT PEER-REVIEWED | Posted: 1 May 2023 doi:10.20944/preprints202305.0012.v1

different segments of the small intestine. As shown in Figure 6, there was a significant decrease in E-cadherin protein expression in the jejunum and ileum in BNP infused mice compared to vehicle infused mice. The basal protein levels of E-cadherin in the duodenum were comparable between the groups (Figure 6).

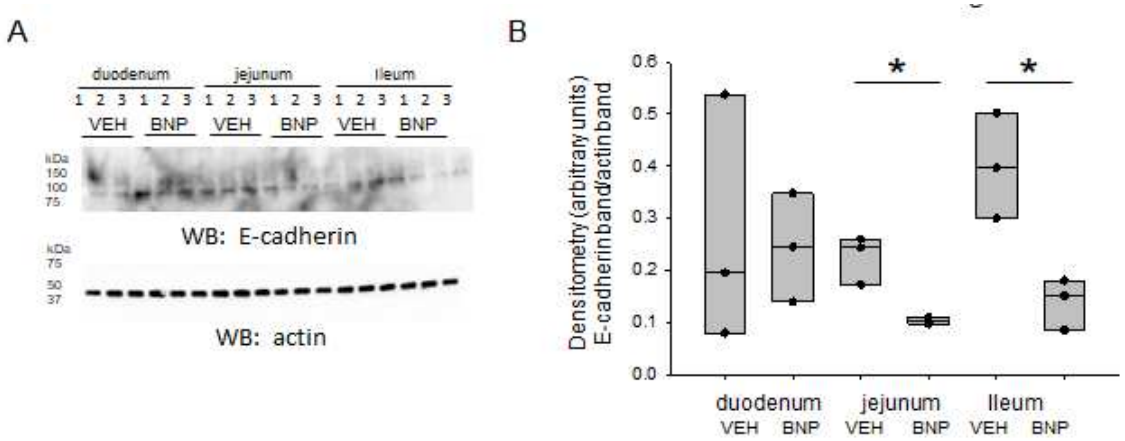

Figure 6. Western blot and densitometric analysis of E-cadherin in the small intestine of mice infused with BNP or vehicle. A. Western blot showing endogenous levels of E-cadherin protein expression (top blot) in the duodenum, jejunum. and ileum and the effect of BNP infusion com-pared to the infusion of vehicle (VEH). Western blot for actin used to assess lane loading. B. Densitometric analysis of the immunoreactive E-cadherin band in the Western blot in panel A normalized to the actin band. * represents a p-value<0.05.

2.6. Kinesin Protein Expression in the Small Intestine is not Altered by BNP Infusion

Additionally, we investigated whether BNP infusion alters kinesin protein expression in different segments of the small intestine. Western blot and densitometric analysis did not reveal any significant changes in kinesin protein expression in any segment of the small intestine after infusion of BNP when compared to vehicle (Figure 7).

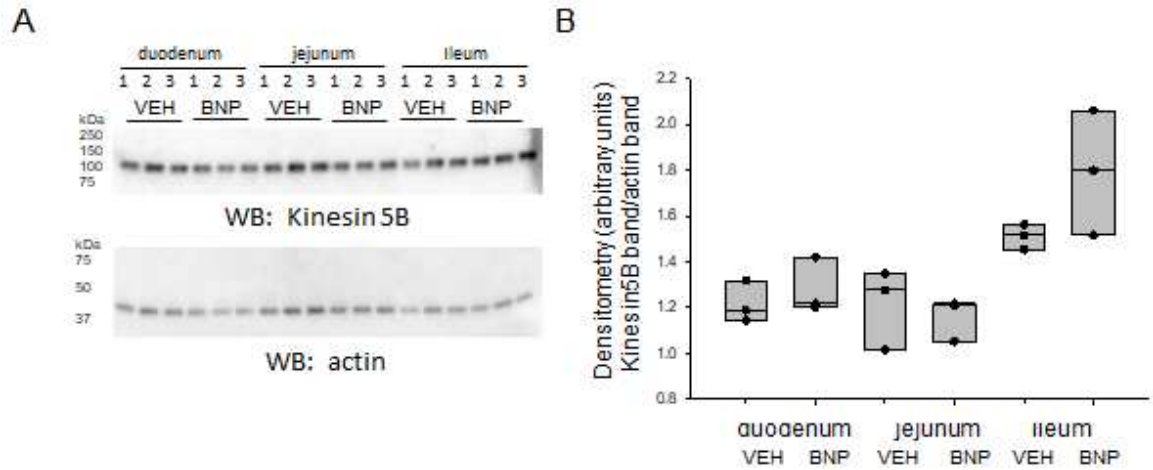

Figure 7. Western blot and densitometric analysis of kinesin 5B in the small intestine of mice infused with BNP or vehicle. A. Western blot showing endogenous levels of kinesin protein expression (top blot) in the duodenum, jejunum. and ileum of mice infused with BNP or vehicle (VEH). Western blot for actin used to assess lane loading. B. Densitometric analysis of the immunoreactive kinesin 5B band in the Western blot in panel A normalized to the actin band.

 doi:10.20944/preprints202305.0012.v1

3. Discussion

Structures necessary for force generation and mechanotransduction such as actin and myosin and their associated proteins are integral components comprising the cytoskeleton of intestinal villi [12,14,28–30]. Even though the mechanism of contraction in the intestinal villi is not very well understood, different studies have reported mechanisms of contraction that are both ATP and calcium dependent with other studies reporting calcium independent mechanisms of contraction [31–33]. One study reported contraction at the tight junctions but not of the microvilli themselves [12].

Our immunostaining fluorescence images show that the localization of NMMII is increased along the crypt and core of the villi in intestinal tissue from BNP treated mice compared to control which may be an indication that the enhanced distribution corresponds to a change in tautness of the villus core which would have an effect on force generation along the tight junction of the microvilli [34]. Our electron micrographic observations indicate BNP treated mice lose the typical 'fanning' or separated appearance that is characteristic of contraction at the crypt region of the intestinal microvilli. A similar appearance was previously shown to be due to contraction at the tight junction regions involving a circumferential contractile ring [14]. Tight junction contraction in turn results in increased paracellular permeability [13,29,35]. Therefore our electron micrographic observation showing decreased contraction of the contractile ring at the tight junction in BNP treated mice supports the hypothesis that BNP makes the tight junctions of intestinal villi less permeable to water and small molecular weight solutes.

Our Western blot and densitometric analyses showed non-muscle myosin and E-cadherin are significantly attenuated in the small intestine of BNP infused mice compared to mice infused with vehicle. E cadherin are integral part of the actin belt (sarcomere belt) at the AJC; and are involved in mechano-transduction and modulation of epithelial cell polarity and shape [36–38]. Theses mechanical effects in turn have been shown to influence paracellular permeability. Western blot and densitometric analysis showed alpha smooth muscle actin and kinesin proteins in the different segments of the small intestine were unaffected by BNP infusion.

E-cadherin plays a critical role in maintaining structural integrity, polarity and contractility of the tight junctions [39–41]. Our prior studies have shown that BNP decreased intestinal absorption in the whole animal mouse model [22,23]. The observation from this current study of reduced expression and differential localization of NMMII and E-cadherin that was observed in intestinal tissue from BNP infused mice compared to vehicle points to at least one of the potential mechanisms for the effect of BNP on gastrointestinal tissue. Transcellular transport of electrolytes and nutrients (e.g., sodium and glucose) is generally an active process involving gradient differences and carriers such as the sodium glucose co-transporter (SGLT1) and it is accompanied by increased tight junction permeability to small solutes [35]. Physiologically such coordination between the transcellular and paracellular pathways of absorption would confer homeostatic advantage; as it would allow regulated (transporter mediated) absorption while directing water and small solutes to the tight junction. Utilizing BNP (and possibly the other natriuretic peptides) for this process would have homeostatic benefits; especially in states when there is a need to regulate total body volume as in the case of heart failure, by decreasing free paracellular movement of water while still permitting apical transport of nutrients. Although the effect of BNP and natriuretic peptides in general on permeability of intestinal epithelia has not been extensively studied in the past, it is known that natriuretic peptides have an effect on permeability of other epithelia such as the vascular endothelium [42–45]. Studies that have looked into this effect of ANP and BNP on permeability of pulmonary vascular epithelium have shown that these effects were at least partially reproduced by cGMP or cGMP analogs [46–49]. A more direct effect that is independent of cGMP was also shown for ANP [45]. Similarly, other studies that have investigated the effect of ANP on counteracting the inflammation associated endothelial permeability have shown that this effect is mediated by NPR-A and cGMP and it is targeted at cytoskeletal actin organization [50,51]. To our knowledge, this is the first study investigating the differences in regional protein expression and relative changes of non-muscle myosin and associated proteins in mouse intestinal tissue after infusion with BNP compared to

 doi:10.20944/preprints202305.0012.v1

vehicle. Although more research needs to be done in this area, our immunostaining and electron micrographic imaging, as well as biochemical data coupled with what is previously known about epithelial tight junction function lends enough support to our hypothesis that BNP has an effect on the contractile structures of intestinal microvilli and that these findings are associated with decreased paracellular permeability. Moreover, further elucidation of the specific mediators and signaling mechanisms for the observed effect of BNP could lead to the identification of novel therapeutic targets for various disease states such as heart failure where volume regulation, and modulating gastrointestinal fluid and electrolyte absorption is crucial.

4. Materials and Methods

Animals

Wild-type (C57BL/6) mice 8-12 weeks of age were purchased from Jax labs. The mice weighed 18-26 grams at the time of the experiment. BNP was purchased from Phoenix pharmaceuticals (Rat, BNP-32, Phoenix Pharmaceuticals, 011–14, Lot # 421752) and was dissolved in modified Krebs solution (vehicle). The vehicle was used as a negative control.

Wild-type (WT) C57BL/6 mice were given a bolus of BNP at 10 ng/g body weight in 100 µl of vehicle followed by infusion of BNP at 1ng/g for 30 minutes. As a control, a group of mice were given 100 µl of vehicle followed by an infusion of equal volume of vehicle for 30 minutes. After the 30-minute infusion, the mice were euthanized and intestinal tissue removed and sectioned into, duodenum, jejunum, and ileum following anatomical demarcations.

Immunostaining

Gastric and intestinal tissue was fixed in 4% paraformaldehyde overnight at 4°C and washed with phosphate buffered saline (PBS) for 15 minutes twice at room temperature with gentle rocking. The tissues were then subject to dehydration and permeabilization by placing them in ascending concentrations of 30, 50 and 70 % methanol each for 15 minutes. Then the tissues were placed in a solution composed of 100 % methanol: DMSO: 30% H_2O_2 prepared at a ratio of 4:1:1. The tissue was left in this solution overnight at 4°C and washed the next morning in 70% methanol for 30 minutes at room temperature with gentle rocking. Rehydration was accomplished by serially placing the tissue in 70% methanol/PBS for 30 minutes while rocking, 50% of methanol/PBS while rocking, 1 ml of 1XPBS for 30 minutes while rocking, 1 ml of PBSMT (PBS, milk, Tween 20) for 30 minutes with rocking twice before the tissue was incubated overnight with 1 ml of primary antibody diluted in PBSMT (1:250) with rocking at 4 °C. The next morning the tissue is rinsed with PBSMT 2x with 1 ml for 1 hour at 4°C, 4 x in 1 ml for 1 hour each at room temperature. Next the tissue is incubated overnight with 1 ml of the secondary antibody diluted in PBSMT (1:250) at 4°C while rocking and washed as described above with PBSMT and rinsed with PBT (PBS and Tween -20 equal concentration). Post fixing was performed in 4% paraformaldehyde in PBS at 4° C overnight. Dehydration was performed in the following sequence: 1 ml of PBT quick rinse, 1ml PBT for 30 minutes at room temperature, 1 ml 50 % methanol for 30 minutes, 1 ml of 70 % methanol for 30 minutes at room temperature; 1 ml of 100 % methanol 30 minutes at room temperature twice. Plastic embedding was achieved by transferring the tissue from 100% methanol to araldite embedding medium and kept in medium for 3 hours. The tissue was then transferred into a fresh embedding medium into a mold on araldite rafts and the mold was kept overnight in a 60° C oven to allow the araldite to harden. The hardened plastic embedded tissue was then trimmed and sectioned using a microtome at 1-3 µm thickness. The sections were passed automatically into water, are transferred onto a slide and allowed to dry for 5-10 minutes on the surface of a hot plate. The first and last section were placed on one side and stained with toluidine blue to guide orientation. Details of the above technique and protocol are described by Linask and Tsuda [27]. Fluorescence imaging was obtained using a Nikon Optiphot II microscope.

 doi:10.20944/preprints202305.0012.v1

SDS-PAGE and Western blotting

Regional protein expression was examined from freshly isolated mice intestinal tissue obtained from mice infused with either BNP or vehicle. Briefly, isolated whole tissue sections of the stomach, duodenum, jejunum, and ileum were homogenized in tissue protein extraction reagent (TPER) (Thermo Scientific) supplemented with protease and phosphatase inhibitors (Thermo Scientific). A BCA assay was performed to determine protein concentration. Eighty micrograms of total protein per lane was resolved on 4-20% gradient sodium dodecyl sulfate polyacrylamide gels at 200V for one hour. The proteins were electrically transferred onto nitrocellulose membranes for immunoblotting. The membranes were blocked in 5% non-fat dry milk in Tris Buffered Saline (TBS) (BIO RAD) before being probed with specific primary antibodies (anti-non muscle myosin heavy chain II-B (BioLegend; San Diego, CA), anti-alpha smooth muscle actin (BioLegend; San Diego, CA), anti-kinesin 5B (Novus Biologicals (Centennial, CO), anti-E-cadherin (Cell Signaling Tech; Danvers, MA) each prepared at a 1:1000 dilution in 5% bovine serum albumin (BIO RAD) TBS. After a series of three washes with 1XTBS, the membranes were incubated with anti-mouse, anti-rat, or anti-rabbit (BIO RAD) secondary antibody prepared at a dilution of 1:3000 in 5% non-fat dry milk in 1XTBS. After extensively washing the membranes four times with 1XTBS, the membranes were incubated with ECL reagent (BioRad) and then developed using an imaging system (BioRad). The band intensities from the Western blots were quantified with NIH Image J software and the signals were normalized to beta actin.

Electron microscopy

Tissue samples (BNP treated vs. control) were fixed on ice, immediately after dissection, in a 2.5% glutaraldehyde–2.0% para-formaldehyde solution containing 0.1 M cacodylate buffer (pH 7.4). Samples were postfixed in cacodylate-buffered 1% OsO_4 for 2 h at 4°C. After dehydration in graded alcohol, tissue pieces were embedded in a mixture of eponaraldite. Ultrathin sections were stained with uranyl acetate and lead citrate and were imaged on the Hitachi H-7000 electron microscope in transmission mode. Transmission Electron Microscopy (TEM) imaging was done at the USF, School of Public Health electron microscopy facility. Tissue section that was not treated with the first antibody was used as a methodological control to evaluate the potential of nonspecific binding.

Statistical Analysis

Data is presented as mean values ± SEM. SigmaPlot software (Jandel Scientific, CA, USA) was used to plot the data and to perform a student t-test for determining statistically significances between the two groups.

Author Contributions: A.A., Y.E.D., D.M., L.A and A.A.A. performed experiments and analyzed data. A.A. and A.A.A. were involved in the supervision of this study, provided resources, and acquired funding for this project. A.A. and A.A.A. were involved in the writing and editing of this manuscript.

Funding: This work was supported by a National Institute of Diabetes and Digestive and Kidney Diseases Grant R01 DK123078 (to AAA).

Institutional Review Board Statement: All animal studies were performed under an approved Institutional Animal Care and Use Committee protocol (IACUC Study #202011157; approved 12/11/2020) at the University of Florida.

Informed Consent Statement: Not applicable.

Data Availability Statement: The individual data points from each experiment are plotted and shown within the figures of this manuscript.

Acknowledgments: We would like to thank Dr. Truitt Sutton for his assistance with electron microscopy and Dr. Keristi Linask and Dr. Mingda Han for their assistance with the immunostaining.

Conflicts of Interest: The authors declare no conflict of interest.

References

1. Sellers JR. Myosins: a diverse superfamily. Biochim Biophys Acta. 2000; 1496: 3-22.
2. Bresnick AR. Molecular mechanisms of nonmuscle myosin-II regulation. Curr Opin Cell Biol. 1999; 11: 26-33.
3. Conti MA and Adelstein RS. Nonmuscle myosin II moves in new directions. J Cell Sci. 2008; 121: 11-8.
4. Heissler SM and Manstein DJ. Nonmuscle myosin-2: mix and match. Cell Mol Life Sci. 2013; 70: 1-21.
5. Beach JR and Hammer JA, 3rd. Myosin II isoform co-assembly and differential regulation in mammalian systems. Exp Cell Res. 2015; 334: 2-9.
6. Thomas DG, Yenepalli A, Denais CM, et al. Non-muscle myosin IIB is critical for nuclear translocation during 3D invasion. J Cell Biol. 2015; 210: 583-94.
7. Ebrahim S, Fujita T, Millis BA, et al. NMII forms a contractile transcellular sarcomeric network to regulate apical cell junctions and tissue geometry. Curr Biol. 2013; 23: 731-6.
8. Woichansky I, Beretta CA, Berns N and Riechmann V. Three mechanisms control E-cadherin localization to the zonula adherens. Nat Commun. 2016; 7: 10834.
9. Drenckhahn D and Dermietzel R. Organization of the actin filament cytoskeleton in the intestinal brush border: a quantitative and qualitative immunoelectron microscope study. J Cell Biol. 1988; 107: 1037-48.
10. Ivanov AI, Hunt D, Utech M, Nusrat A and Parkos CA. Differential roles for actin polymerization and a myosin II motor in assembly of the epithelial apical junctional complex. Mol Biol Cell. 2005; 16: 2636-50.
11. Shen L, Black ED, Witkowski ED, et al. Myosin light chain phosphorylation regulates barrier function by remodeling tight junction structure. J Cell Sci. 2006; 119: 2095-106.
12. Keller TC, 3rd and Mooseker MS. Ca++-calmodulin-dependent phosphorylation of myosin, and its role in brush border contraction in vitro. J Cell Biol. 1982; 95: 943-59.
13. Hecht G, Pestic L, Nikcevic G, et al. Expression of the catalytic domain of myosin light chain kinase increases paracellular permeability. Am J Physiol. 1996; 271: C1678-84.
14. Broschat KO, Stidwill RP and Burgess DR. Phosphorylation controls brush border motility by regulating myosin structure and association with the cytoskeleton. Cell. 1983; 35: 561-71.
15. Shen L, Weber CR, Raleigh DR, Yu D and Turner JR. Tight junction pore and leak pathways: a dynamic duo. Annu Rev Physiol. 2011; 73: 283-309.
16. Bu Y, Wang N, Wang S, et al. Myosin IIb-dependent Regulation of Actin Dynamics Is Required for N-Methyl-D-aspartate Receptor Trafficking during Synaptic Plasticity. J Biol Chem. 2015; 290: 25395-410.
17. Alli AA, Bao HF, Alli AA, et al. Phosphatidylinositol phosphate-dependent regulation of Xenopus ENaC by MARCKS protein. Am J Physiol Renal Physiol. 2012; 303: F800-11.
18. Alli AA, Bao HF, Liu BC, et al. Calmodulin and CaMKII modulate ENaC activity by regulating the association of MARCKS and the cytoskeleton with the apical membrane. Am J Physiol Renal Physiol. 2015; 309: F456-63.
19. Reifenberger MS, Yu L, Bao HF, et al. Cytochalasin E alters the cytoskeleton and decreases ENaC activity in Xenopus 2F3 cells. Am J Physiol Renal Physiol. 2014; 307: F86-95.
20. Glotfelty LG, Zahs A, Iancu C, Shen L and Hecht GA. Microtubules are required for efficient epithelial tight junction homeostasis and restoration. Am J Physiol Cell Physiol. 2014; 307: C245-54.
21. Ivanov AI, McCall IC, Babbin B, Samarin SN, Nusrat A and Parkos CA. Microtubules regulate disassembly of epithelial apical junctions. BMC Cell Biol. 2006; 7: 12.
22. Addisu A, Gower WR, Jr., Landon CS and Dietz JR. B-type natriuretic peptide decreases gastric emptying and absorption. Exp Biol Med (Maywood). 2008; 233: 475-82.
23. Addisu A, Gower WR, Jr., Serrano M, Villarreal D and Dietz JR. Heart failure mice exhibit decreased gastric emptying and intestinal absorption. Exp Biol Med (Maywood). 2011; 236: 1454-60.
24. Takagi K and Araki N. Relaxant effects of brain natriuretic peptide on guinea-pig tracheal smooth muscle. Clin Exp Pharmacol Physiol. 1993; 20: 239-43.
25. Guo HS, Cai ZX, Zheng HF, et al. Role of calcium-activated potassium currents in CNP-induced relaxation of gastric antral circular smooth muscle in guinea pigs. World J Gastroenterol. 2003; 9: 2054-9.
26. Protter AA, Wallace AM, Ferraris VA and Weishaar RE. Relaxant effect of human brain natriuretic peptide on human artery and vein tissue. Am J Hypertens. 1996; 9: 432-6.
27. Linask KK and Tsuda T. Application of plastic embedding for sectioning whole-mount immunostained early vertebrate embryos. Methods Mol Biol. 2000; 135: 165-73.
28. Rostgaard J. Electron microscopy of filaments in the basal part of rat kidney tubule cells, and their in situ interaction with heavy meromyosin. Z Zellforsch Mikrosk Anat. 1972; 132: 497-521.
29. Tilney LG and Mooseker MS. Actin filament-membrane attachment: are membrane particles involved? J Cell Biol. 1976; 71: 402-16.
30. Mooseker MS. Brush border motility. Microvillar contraction in triton-treated brush borders isolated from intestinal epithelium. J Cell Biol. 1976; 71: 417-33.

31. Swanljung-Collins H and Collins JH. Ca2+ stimulates the Mg2(+)-ATPase activity of brush border myosin I with three or four calmodulin light chains but inhibits with less than two bound. J Biol Chem. 1991; 266: 1312-9.
32. Swanljung-Collins H and Collins JH. Rapid, high-yield purification of intestinal brush border myosin I. Methods Enzymol. 1991; 196: 3-11.
33. Swanljung-Collins H and Collins JH. Phosphorylation of brush border myosin I by protein kinase C is regulated by Ca(2+)-stimulated binding of myosin I to phosphatidylserine concerted with calmodulin dissociation. J Biol Chem. 1992; 267: 3445-54.
34. Burgess DR. Reactivation of intestinal epithelial cell brush border motility: ATP-dependent contraction via a terminal web contractile ring. J Cell Biol. 1982; 95: 853-63.
35. Turner JR, Rill BK, Carlson SL, et al. Physiological regulation of epithelial tight junctions is associated with myosin light-chain phosphorylation. Am J Physiol. 1997; 273: C1378-85.
36. Bertet C, Sulak L and Lecuit T. Myosin-dependent junction remodelling controls planar cell intercalation and axis elongation. Nature. 2004; 429: 667-71.
37. Cai Y, Biais N, Giannone G, et al. Nonmuscle myosin IIA-dependent force inhibits cell spreading and drives F-actin flow. Biophys J. 2006; 91: 3907-20.
38. Fernandez-Gonzalez R, Simoes Sde M, Roper JC, Eaton S and Zallen JA. Myosin II dynamics are regulated by tension in intercalating cells. Dev Cell. 2009; 17: 736-43.
39. Braga V. Spatial integration of E-cadherin adhesion, signalling and the epithelial cytoskeleton. Curr Opin Cell Biol. 2016; 42: 138-45.
40. Biswas KH and Zaidel-Bar R. Early events in the assembly of E-cadherin adhesions. Exp Cell Res. 2017.
41. Gumbiner B. Cadherins: a family of Ca2+-dependent adhesion molecules. Trends Biochem Sci. 1988; 13: 75-6.
42. He P, Zeng M and Curry FE. cGMP modulates basal and activated microvessel permeability independently of [Ca2+]i. Am J Physiol. 1998; 274: H1865-74.
43. Huxley VH, Tucker VL, Verburg KM and Freeman RH. Increased capillary hydraulic conductivity induced by atrial natriuretic peptide. Circ Res. 1987; 60: 304-7.
44. Lofton CE, Newman WH and Currie MG. Atrial natriuretic peptide regulation of endothelial permeability is mediated by cGMP. Biochem Biophys Res Commun. 1990; 172: 793-9.
45. Kubes P. Nitric oxide-induced microvascular permeability alterations: a regulatory role for cGMP. Am J Physiol. 1993; 265: H1909-15.
46. Westendorp RG, Draijer R, Meinders AE and van Hinsbergh VW. Cyclic-GMP-mediated decrease in permeability of human umbilical and pulmonary artery endothelial cell monolayers. J Vasc Res. 1994; 31: 42-51.
47. Draijer R, Atsma DE, van der Laarse A and van Hinsbergh VW. cGMP and nitric oxide modulate thrombin-induced endothelial permeability. Regulation via different pathways in human aortic and umbilical vein endothelial cells. Circ Res. 1995; 76: 199-208.
48. Klinger JR, Warburton R, Carino GP, et al. Natriuretic peptides differentially attenuate thrombin-induced barrier dysfunction in pulmonary microvascular endothelial cells. Exp Cell Res. 2006; 312: 401-10.
49. Holschermann H, Noll T, Hempel A and Piper HM. Dual role of cGMP in modulation of macromolecule permeability of aortic endothelial cells. Am J Physiol. 1997; 272: H91-8.
50. Kiemer AK, Kulhanek-Heinze S, Gerwig T, Gerbes AL and Vollmar AM. Stimulation of p38 MAPK by hormonal preconditioning with atrial natriuretic peptide. World J Gastroenterol. 2002; 8: 707-11.
51. Kiemer AK, Weber NC, Furst R, Bildner N, Kulhanek-Heinze S and Vollmar AM. Inhibition of p38 MAPK activation via induction of MKP-1: atrial natriuretic peptide reduces TNF-alpha-induced actin polymerization and endothelial permeability. Circ Res. 2002; 90: 874-81.